

In vitro dermal penetration of nickel nanoparticles

Matteo Crosera^{a, b}, Gianpiero Adami^a, Marcella Mauro^b, Massimo Bovenzi^b,
Elena Baracchini^a, Francesca Larese Filon^{b, *}

^a Department of Chemical and Pharmaceutical Sciences, University of Trieste, Via L. Giorgieri 1, 34127, Trieste, Italy

^b Department of Medical Sciences, University of Trieste, Via della Pietà 1, 34129, Trieste, Italy

H I G H L I G H T S

- NiNPs applied on the skin caused penetration of Ni inside the skin and permeation through the skin.
- Ni absorption was significantly higher when a damaged skin protocol has been used.
- Small amount of NiNPs could lead to a higher absorption of Ni compared to bulk materials.
- Preventive measures are needed when NiNPs are produced and used.

A R T I C L E I N F O

Accepted 21 November 2015

Keywords:

Nanoparticles
In vitro
Skin penetration
Damaged skin
Nickel

A B S T R A C T

Nickel nanoparticles (NiNPs) represent a new type of occupational exposure because, due to the small size/high surface, they can release more Ni ions compared to bulk material. It has been reported a case of a worker who developed sensitization while handling nickel nanopowder without precautions. Therefore there is the need to assess whether the skin absorption of NiNPs is higher compared to bulk nickel.

Two independent *in vitro* experiments were performed using Franz diffusion cells. Eight cells for each experiment were fitted using intact and needle-abraded human skin. The donor phase was a suspension of NiNPs with mean size of 77.7 ± 24.1 nm in synthetic sweat.

Ni permeated both types of skin, reaching higher levels up to two orders of magnitude in the damaged skin compared to intact skin (5.2 ± 2.0 vs 0.032 ± 0.010 $\mu\text{g cm}^{-2}$, $p = 0.006$) at 24 h. Total Ni amount into the skin was 29.2 ± 11.2 $\mu\text{g cm}^{-2}$ in damaged skin and 9.67 ± 2.70 $\mu\text{g cm}^{-2}$ in intact skin (mean and SD, $p = 0.006$). Skin abrasions lead to doubling the Ni amount in the epidermis and to an increase of ten times in the dermis.

This study demonstrated that NiNPs applied on skin surface cause an increase of nickel content into the skin and a significant permeation flux through the skin, higher when a damaged skin protocol was used. Preventive measures are needed when NiNPs are produced and used due to their higher potential to enter in our body compared to bulk nickel.

1. Introduction

In industrialized countries, skin is at high risk of exposure to chemicals and other contaminants, which can be found in the environment and at a workplace. Contact allergy affects approximately 20% of the general population (Thyssen et al., 2009) and nickel (Ni) is recognized as one of the most common cause of contact dermatitis affecting millions of people worldwide (Rui

A wide variety of metal objects, which come into repetitive contact with the skin, can release Ni ions that can diffuse through the skin and cause allergy (Flint, 1998). It is well demonstrated that, under physiologically conditions, nickel in metallic form may ionize and so permeate through the skin: cutaneous nickel exposure may result from wearing or handling jewels, coins, or utensils containing nickel (Liden and Carter, 2001; Liden et al., 2008, Midander et al., 2014; Thyssen et al., 2012). Also nickel powders, both metal and metal oxide, can release nickel ions once they have been immersed in artificial sweat (Midander et al., 2007; Mazinianian et al., 2013).

* Corresponding author. Department of Medical Sciences, University of Trieste, UCO Medicina del Lavoro Via della Pietà 19 34129 Trieste Italy.

E-mail address: larese@units.it (F. Larese Filon).

More extensive studies of nickel skin absorption have been undertaken. It was found that water solution of nickel salts can pass through the stratum corneum in in-vitro system (Tanojo et al., 2001), and nickel powder can penetrate in depth profiles of the stratum corneum after occlusion in in-vivo experiments (Hostynek et al., 2001). The presence of skin abrasions can increase nickel permeation when the skin is exposed to nickel powder in an in-vitro diffusion system (Larese Filon et al., 2009).

Actually, metal, metal oxide and metal alloy nanoparticles represent a group of promising materials useful in several areas as chemical and photochemical catalysis, magnetic materials, micro-electronics, medical imaging, among others.

In particular, nickel nanoparticles (NiNPs) are emerging for many characteristics such as a high level of surface energy, high magnetism, low melting point, high surface area, and low burning point. For these characteristics their use has been proposed in high magnetic tapes, conducting pastes, chemical catalysis, adjuvant for enhancing immune responses to protein-based vaccines, micro-filters, gas sensing equipment, combustion promotion, super-capacitor electrode material, and light absorbance (Alonso et al., 2010; Ansaldo et al., 2008; Patel et al., 2007; Wu et al., 2012).

Magaye and Zhao (2012) summarized the current knowledge on the genotoxicity and carcinogenicity potential of metallic nickel and nickel-based nanoparticles in *in vitro* and *in vivo* mammalian studies. The NiNPs, due to their small size/high surface, are able to enter human body in more efficient way than bulk nickel, moreover they can release more Ni ions, causing an increase of metal penetration. Recently a case of a 26-years-old female chemist, that developed nickel sensitization with respiratory and skin effects while handling nickel nanopowder with no protective measures, has been reported (Journey and Goldman, 2014).

To investigate the potential nickel skin absorption after exposure to a commercially available nickel nanopowder, a series of *in vitro* permeation experiments with human skin has been carried out using the Franz static diffusion cell method (Franz, 1975). Experiments have been performed using intact as well as damaged skin to estimate the effect of skin lesions on skin absorption. The experience and the protocols employed during the European project EDETOX (Evaluations and predictions of Dermal absorption of TOXic chemicals), a three-year research program (2001–2004) funded by European Union (Sandt et al., 2004) and already used to testing the skin absorption of other metal nanoparticles such as gold, cobalt, platinum and rhodium nanoparticles (Larese Filon et al., 2011, 2013; Mauro et al., 2015) was used.

2. Materials and methods

2.1. Chemicals

All chemicals were analytical graded. Magnesium nitrate, urea, sodium chloride, sodium hydrogenphosphate, potassium dihydrogenphosphate, were purchased from Carlo Erba (Milan, Italy); lactic acid (90% v/v) was bought from Acros Organics (Geel, Belgium); nitric acid (69.5% v/v), hydrogen peroxide (30% v/v), hydrochloric acid (36.5–38% v/v), ammonium hydroxide (25% w/v) from Sigma Aldrich (Milan, Italy).

Ni nanopowder (CAS 7440-02-0) came from Sigma Aldrich (Milan, Italy), APS (Average Particle Size) < 100 nm, purity $\geq 99.9\%$ trace metals basis).

Water reagent grade was produced with a Millipore purification pack system (milliQ water).

2.2. Preparation of the donor phase

The donor phase has been prepared just before the experiment:

100 mg of Ni nanopowder were dispersed by sonication for 10 min in 100 mL of synthetic sweat at pH 4.5. The synthetic sweat solution included 0.5% sodium chloride, 0.1% urea and 0.1% lactic acid in milliQ water; pH 4.5 was adjusted with ammonia. The total nickel concentration (1.0 g L^{-1} of the donor solution) has been confirmed by Inductively Coupled Plasma – Atomic Emission Spectroscopy (ICP-AES) analyses.

Once they have been dispersed in synthetic sweat and at the end of the experiments, NiNPs have been also visualized by means of Transmission Electron Microscopy (TEM).

At the time of the experiments, NiNPs have been removed from aqueous solution in three different aliquots (2 mL) of the freshly prepared solution by means of ultrafiltration in centrifuge at 5000 rpm for 30 min using the Amicon Ultra-4 centrifugal filters (10 K MWCO) in order to evaluate the percentage of ionized metal in the donor phase. The filtered solutions have been collected and analysed for determining the concentrations by means of ICP-AES.

The ionization of the donor phase has been checked also after the 24-h exposure, repeating the ultrafiltration procedure on the donor phases, once they have been removed from the cells at the end of the experiments.

2.3. Preparation of skin membranes

Human abdominal full thickness skin was obtained as surgical waste after the authorization of the local Ethical Committee and it was used for the absorption experiments immediately after the surgical operations. After the skin excision, subcutaneous fat was removed and hair shaved by a razor. From each skin specimen, $4 \times 4 \text{ cm}^2$ pieces were cut and mounted separately on the diffusion cells, that were previously washed a first time with freshly prepared Aqua Regia, a second time with diluted nitric acid and rinsed three times with milliQ water.

Skin integrity has been tested before and after the experiments using electrical conductivity by means of a conductometer (Metrohm, 660, Metrohm AG Oberdorfstr. 68 CH-9100 Herisau) operating at 300 Hz and connected to two stainless steel electrodes (Fasano et al., 2002). The conductivity data in μS were converted into $\text{K}\Omega \text{ cm}^{-2}$. Cells with a resistance lower than $3.95 \pm 0.27 \text{ k}\Omega \text{ cm}^{-2}$ were considered to be damaged and rejected as suggested by Davies et al. (2004).

2.4. In vitro diffusion system

Percutaneous absorption studies were performed using static diffusion cells following the Franz method (Franz, 1975). The receptor compartment had a mean volume of 14.0 mL and was maintained at $32 \text{ }^\circ\text{C}$ by means of circulation of thermostated water in the jacket surrounding the cell. This temperature value was chosen in order to reproduce physiological temperature of the hand at normal conditions.

The physiological solution used as receptor fluid has been prepared by dissolving 2.38 g of Na_2HPO_4 , 0.19 g of KH_2PO_4 and 9 g of NaCl into 1 L of milliQ water (final pH = 7.35). The concentration of the salts in the receptor fluid was approximately the same of the human blood. The receiving solution in each cell was continuously stirred using a Teflon coated magnetic stirrer.

Each piece of skin was clamped between the donor and the receptor chambers; the mean exposed skin area was 3.29 cm^2 and the average membranes thickness was 1.1 mm.

The experiments were carried out as follows:

Experiment 1: At time 0, the exposure chambers of 4 Franz diffusion cells were filled with 2.0 mL of the donor solution (0.6 mg cm^{-2}) to ensure an infinite dose. The applied dose was the same of previous studies in order to better compare the results of

the experiments as summarised in [Larese Filon et al. \(2015\)](#). At selected intervals (4, 8, 16, 24 h) 1.5 mL of the dermal bathing solution has been removed and stored in freezer for the following analyses. Each receptor sample was immediately replaced with an equal volume of fresh physiological solution.

After 24 h the donor phase of each diffusion cell has been removed and recovered for the following analysis; after the integrity test, also the receiving solutions and the skin pieces have been removed and stored in the freezer for the quantitative analyses.

The total nickel concentrations of the donor phases were confirmed after the experiments by means of Inductively Coupled Plasma-Atomic Emission Spectroscopy (ICP-AES).

Experiment 2: experiment 1 has been repeated using an abraded skin protocol as suggested by [Bronaugh and Steward \(1985\)](#) and adapted by [Larese Filon et al. \(2006\)](#); skin pieces have been abraded by drawing the point of a 19-gauge hypodermic needle across the surface (20 marks in one direction and 20 perpendicular).

Blanks: for each experiment, two cells were added as blank. The blank cells were treated as the others with the exception that synthetic sweat, without NiNPs, has been introduced as donor phase.

Each experiment has been repeated two times, in order to use the skin of four different donors. As the equipment used was static, there is no relationship between the cells tested, hence each of them represents an independent evaluation, for a total of 8 cells with intact skin, 8 cells with damaged skin, and 8 blank cells.

Donors were healthy men and women with a range of age from 50 to 75.

2.5. Skin content evaluation

After the experiments the skin pieces were removed from the diffusion cells, accurately rinsed with milliQ water to remove residual NiNPs from the skin surface. The exposed area of each piece of skin has been cut with a surgical scissor, and finally has been separated into epidermis and dermis by heat shock immersing them in water at 60 °C for 1 min.

All the skin fractions have been collected and stored individually in freezer at -25 °C. At the time of the analysis, the skin membranes have been dried for 2 h at room temperature, then cut into sections and put into beakers with 10 mL of HNO₃ 69% v/v for digestion (amounts of skin were 0.96 ± 0.20 g). They were agitated at room temperature over night and then heated at the boiling point (after 2 h they were added, drop by drop, of 2 mL of H₂O₂ 30% v/v) till the solution volumes were approximately of 2 mL. The solutions were diluted to a final volume of 10 mL with milliQ water for the ICP-AES analyses.

2.6. Quantitative analysis

The total nickel concentration measurements of the receiving phases were performed using Electro-Thermal Atomic Absorption Spectrometry (ETAAS) with Zeeman background correction. A Thermo M series AA spectrometer equipped with a GF95Z Zeeman Furnace and a FS95 Furnace Autosampler (Thermo Electron Corporation, Cambridge, UK) were used.

A 2% w/v solution of Mg(NO₃)₂ was used as modifying matrix. The samples were analysed measuring against standard solutions for instrumental calibration. Ni detection limit at the analytical wavelength of 232.0 nm was 0.2 µg L⁻¹. The precision of the measurements as relative standard deviation (RSD%) for the analysis was always less than 5%.

The total nickel concentration in the donor phases and in the solutions resulting from the skin sample mineralization were performed by Inductively Coupled Plasma-Atomic Emission

Spectrometry (ICP-AES) using a Spectroflame Modula E optical plasma interface (OPI) instrument (by SPECTRO, Germany). The analysis were conducted using a calibration curve obtained by dilution (range: 0–10 mg L⁻¹) of Spectrascan[®] Nickel standard solution for ICP-AES analyses (by Teknolab A/S, Norway). The limit of detection (LOD) at the operative wavelength of 231,604 was 0.020 mg L⁻¹. The precision of the measurements as relative standard deviation (RSD%) for the analysis was always less than 5%.

2.7. Data analysis

Ni concentration data (µg cm⁻³) in the receptor solution were converted to the total amount that penetrated through the unit surface area (µg cm⁻²), with a correction for dilution due to sample removal during the sampling procedure, then plotted against time. The slope of this plot in the linear steady-state region gives the flux of Ni through the skin, simple division yielding the rate per cm². Lag time was calculated as the intercept of the curve with X-axis.

Data analysis was performed using the statistical software STATA release 13 (Texas inc.). Data were reported as mean ± standard deviation (SD). The difference between independent data was assessed by means of the Mann-Whitney and Kruskal Wallis tests. A p value of 0.05 was considered as the limit of statistical significance.

2.8. Skin fixation protocol for TEM analysis

After removal, small sections (dimensions: 1 × 1 × 1 mm) were taken from selected skin samples and fixed for 3 h in a solution of 3% glutaraldehyde (Serva, Heildemberg, Germany) in 0.1 M cacodylate buffer (pH 7.3). The fixed sections were washed twice (10 min each) with 0.1 M cacodylate buffer and then post fixed with 1% osmium tetroxide for 1 h at 4 °C. Post-fixed samples were dehydrated with an ascending ethanol series ending to 100% ethanol and then embedded in Down epoxy resin (DER332; Unione Chimica Europea, Milan, Italy) and DER732 (Serva). The last resin embedding was made under vacuum. Semi-fine and ultra-thin sections were prepared with an ultra-microtome Leica Ultracut UCT (Leica Microsystem, Milan, Italy) equipped with a diamond blade Drukker 3 mm (Emme3, Milan, Italy). Semi-fine sections were observed with an optical microscope Leitz Dialux 20 EB (Leica Microsystems, Milan, Italy) instead ultra-thin sections were double stained with lead citrate and uranyl acetate and observed with Transmission Electron Microscope (EM208; Philips, Heildhoven, The Netherlands) with an high definition acquisition system SIS Morada and a digital image acquisition system iTEM (FEI Italia, Milan, Italy).

3. Results

The concentration of 1.0 g L⁻¹ of the starting NiNPs dispersion has been confirmed by the ICP-AES analysis. Representative TEM images of NiNPs, diluted in synthetic sweat, before and after the experiments, and their size distribution, are presented in [Figs. 1a,b, and 2](#), respectively. The mean size of the NPs was 77.7 ± 24.1 nm (number of NP measured = 200), but they tended to form bigger aggregates reaching the micrometer range and they deposited on the skin surface in few minutes.

The nickel concentration in the ultrafiltered donor phase collected at the beginning of the test, after the removal of NiNPs, shown 12.6 ± 2.1% of ionized metal of the starting suspensions and did not significantly change at the end of the experiments.

Ni permeated the intact skin reaching 0.032 ± 0.010 µg cm⁻² at 24 h ([Fig. 3a](#)) and this value is three times greater than that reach in the blank cells (0.010 ± 0.003 µg cm⁻²), p = 0.02.

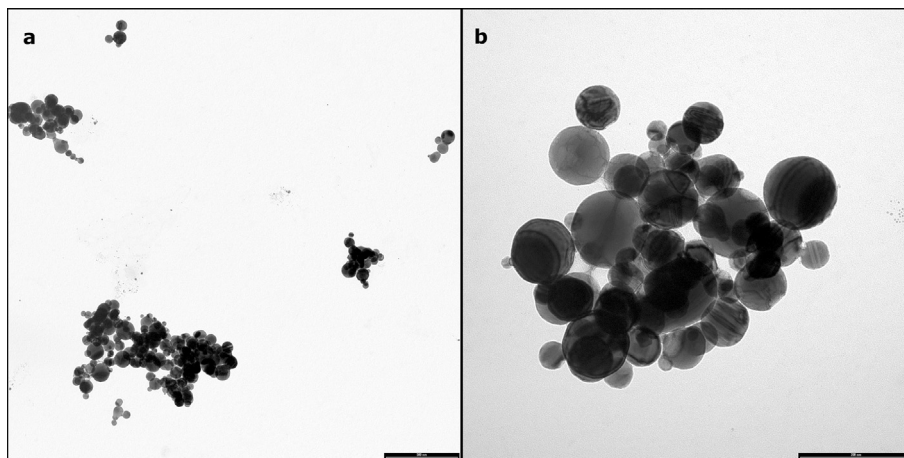


Fig. 1. Representative TEM images of NiNPs aggregates in synthetic sweat (barr a = 500 nm, b = 200 nm).

In damaged skin the Ni absorption significantly ($p = 0.006$) increased of around two orders of magnitude reaching $5.2 \pm 2.0 \mu\text{g cm}^{-2}$ at the end of the exposure time (Fig. 3a). Ni amount found in the receiving solutions was always less than 1% of the NiNPs applied dose. (Fig. 3a,b) confirming that the experiments were conducted in an infinite dose scenario.

Flux through the skin increased of two orders of magnitude comparing intact ($1.7 \pm 0.6 \text{ ng cm}^{-2} \text{ h}^{-1}$) and damaged ($0.30 \pm 0.12 \mu\text{g cm}^{-2} \text{ h}^{-1}$) skin ($p = 0.006$), while a small difference was registered in the lag time values ($6.0 \pm 1.4 \text{ h}$ and 6.6 ± 0.8 , respectively). The total Ni amounts (expressed as $\mu\text{g cm}^{-2}$) penetrated into the dermal layers (epidermis and dermis) for intact and damaged skin, compared to the blank cells values, are summarized in Table 1. As shown in Fig. 4, the Ni amount decreased significantly ($p = 0.01$) from the epidermis to the dermis both in intact and damaged skin and the skin abrasions lead to a doubling of the Ni amount recovered in the epidermis and to an increase of ten times in the dermis.

Finally, TEM investigation on skin exposed samples (Fig. 5a) reveals sporadic formations compatible in size, shape and electron-density with NiNPs in the stratum corneum (Fig. 5b) and in the upper layers of the epidermis (Fig 5c). In the dermis and in the blank tissue samples no NPs have been found.

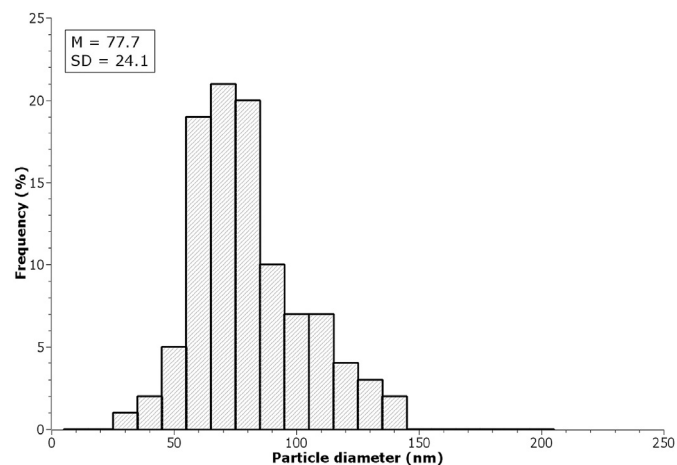


Fig. 2. Size distribution of the NiNPs used in the experiments.

4. Discussion

The applications of nanotechnologies are flooding the market with a number of products containing engineering nanoparticles and the possible applications in the near future seem to be much more greater. Metal NPs represent an important class of these new materials because of the different properties that metals assume at the nanoscale level. At the same time the toxicological evaluation processes are far from to be exhaustive and the exposure of workers and consumers to the new nanomaterials is still a matter of concern.

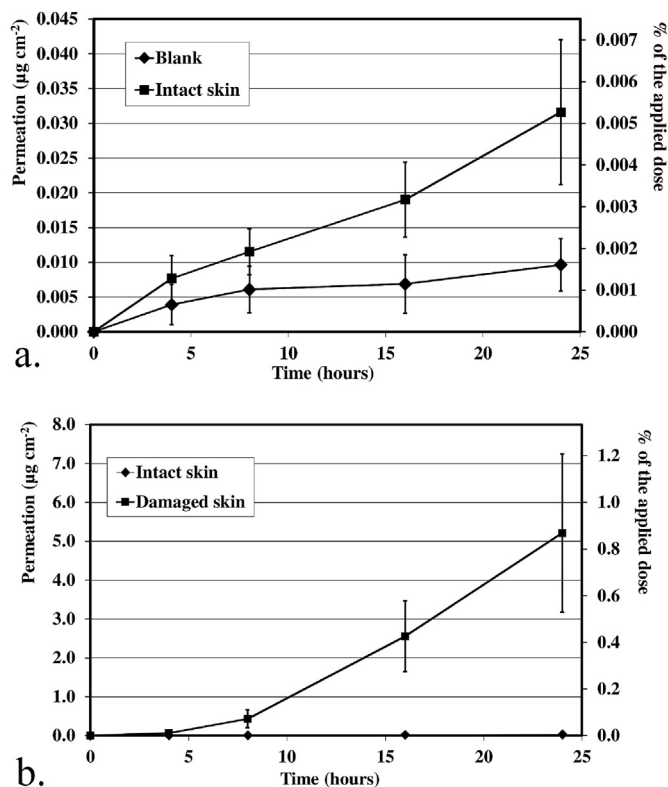


Fig. 3. Permeation profiles of a) blanks and intact skin cells (means and standard deviations); b) damaged skin cells (means and standard deviations). Permeation profiles are expressed against the amount of nickel permeated as $\mu\text{g cm}^{-2}$ (left y-axis) and as the percentage of the applied dose the permeated the skin (right y-axis).

Table 1

Nickel penetrated into the skin layers expressed as $\mu\text{g cm}^{-2}$ (epidermis, dermis, total) in blanks, intact and damaged skin cells (mean \pm standard deviation).

	Blank ($\mu\text{g cm}^{-2}$)	Intact skin ($\mu\text{g cm}^{-2}$)	Damaged skin ($\mu\text{g cm}^{-2}$)
Epidermis	0.24 \pm 0.10	8.86 \pm 2.66*	18.4 \pm 9.2 ^o
Dermis	0.24 \pm 0.05	0.81 \pm 0.27*	10.8 \pm 4.3 ^o
Total	0.49 \pm 0.14	9.67 \pm 2.70*	29.2 \pm 11.2*

*p = 0.02 intact skin vs blanks.

^op = 0.02 damaged skin vs blanks.

^op = 0.006 damaged vs intact skin.

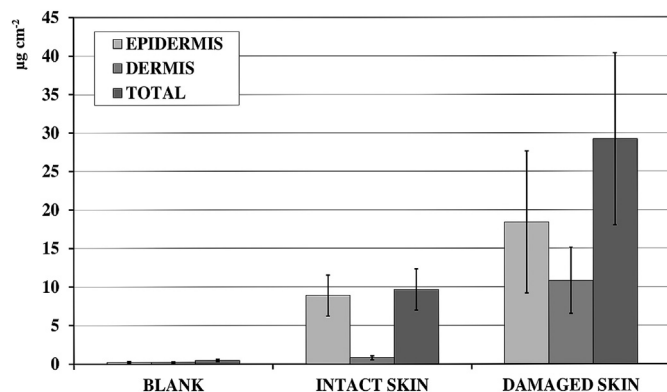


Fig. 4. Mean values and standard deviations of nickel amounts ($\mu\text{g cm}^{-2}$) in epidermis, dermis and total skin, in the three groups of cells (blank, intact and damaged skin).

It is well known that the skin is a route of entry for metals ions after exposure to metal containing objects, metal salts and metal powders (Hostynek, 2003; Larese Filon et al., 2009), and this could be a cause of sensitization and allergic contact dermatitis (Thyssen

and Menné, 2010). In this study the absorption of nickel through intact and damaged human skin after exposure to a commercially available nickel nanopowder has been evaluated using an ex-vivo model. We confirmed that NiNPs applied on the skin surface caused penetration of nickel inside the skin and permeation through the skin, significantly higher when a damaged skin protocol has been used. Our results confirmed the ability of nickel to cross the skin barrier as demonstrated in a previous study in which the skin had been exposed to fine nickel powder with an average particle size (APS) of 2.2–3.0 μm (Larese Filon et al., 2009). Comparison between the two experiments is reported in Table 2.

With respect to the experiments with nickel fine powder in which a dose of 23 mg cm^{-2} , in the present work a dose of 0.6 mg cm^{-2} has been applied: nevertheless the nickel permeation data at the end of the tests are of the same order of magnitude. It means that a dose forty times lower of nickel as nanopowder reached similar receiving solution concentrations than nickel fine powder. Considering the Ni ion concentrations of the donor phases of the two experiments (12.6% for NiNPs and 0.002% for Ni fine powder) it appears that comparable ion doses have been applied (range of 0.02–0.06 mg cm^{-2} for Ni fine powder and of 0.06–0.09 mg cm^{-2} for NiNPs). This considerably higher ionisation is probably due to the higher surface/volume ratio of the nanoparticles respect to the same material in bulk form. Since naked NiNPs tend to form big aggregates in water dispersion and considering that 80 nm NPs seems too big to be absorbed through the skin (Larese Filon et al., 2015), it can be hypothesized that the permeation is most likely due to the ionized metal released from the nanopowder in synthetic sweat. This hypothesis is also confirmed by the low number of NPs visualized during TEM investigation, so the possibility that they are the result of artefacts due to the complex sample preparation cannot be excluded.

Moreover, considering the composition of the synthetic sweat, it might be expected the formation of small, hydrophilic complexes,

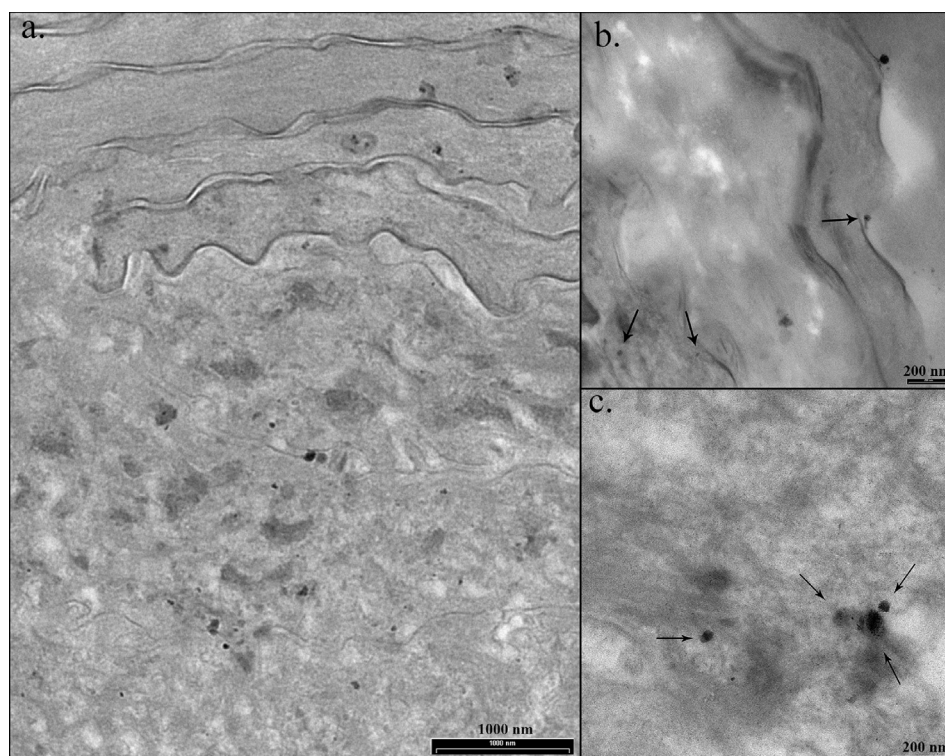


Fig. 5. Representative TEM micrographs of NiNPs-treated skin samples (a) and of NPs in the stratum corneum (b) and in the epidermis (c). Barr: a = 1000 nm, b,c = 200 nm.

Table 2Comparison of nickel permeation data ($M \pm SD$) after exposure to Ni nanopowder and Ni fine powder (from Larese Filon et al., 2009).

	Nickel fine powder (Larese Filon et al., 2009)	Nickel nanopowder
Average particle size	2.2–3 μm	77 nm
Total dose (mg cm^{-2})	23	0.6
Ion dose (mg cm^{-2})	0.02–0.06	0.06–0.09
Receiving Phases Blank ($\mu\text{g cm}^{-2}$)	0.007 ± 0.003	0.010 ± 0.003
Receiving Phases Intact skin ($\mu\text{g cm}^{-2}$)	0.032 ± 0.014	0.032 ± 0.010
Receiving Phases Damaged skin ($\mu\text{g cm}^{-2}$)	3.81 ± 3.41	5.21 ± 2.03

such as chloride or lactate, that mainly pass through the aqueous environment of sweat duct respect to lipophilic intercellular route (Hostynek et al., 2001).

Furthermore, this study confirms the capability of the skin to accumulate nickel ions: in fact, in front of a permeation only three times greater in the intact skin compared to blank, the concentration in the skin is about twenty times greater (forty time if we consider the epidermis). Then the skin, and in particular the epidermis, can act as a reservoir of nickel which could be released over time (Fullerton and Hoelgaard, 1988) and an important role would be played by different factors such as the turnover time of the stratum corneum and the water-soluble forms of the metals in the sweat (Hostynek, 2003). From an exposure point of view, these results raise some concerns about the safety handling of these types of nanomaterials because also a contact with small amount of NiNPs, compared to bulk materials, could lead to a relevant absorption of nickel that can cause sensitization and symptoms in exposed people. Preventive measures are needed when NiNPs are produced and used, due to their higher potential to enter in our body compared to bulk nickel, as dictated by the EU Precautionary Principle (i.e. rapid response in the face of a possible danger to human where scientific data do not permit a complete evaluation of the risk).

References

Alonso, F., Riente, P., Sirvent, J.A., Yus, M., 2010. Nickel nanoparticles in hydrogen-transfer reductions: characterisation and nature of the catalyst. *Appl. Catal. A General* 378, 42–51.

Ansaldò, A., George, C., Parodi, M.T., Di Zitti, E., Roth, S., Ricci, D., 2008. Ex-situ synthesized nickel nanoparticles for multi-walled carbon nanotube growth on high aspect ratio substrates. *Phys. Status Solidi (b)* 245, 1923–1926.

Bronaugh, R.L., Steward, R.F., 1985. Methods for in vitro percutaneous absorption studies V: permeation through damaged skin. *J. Pharm. Sci.* 74, 1062–1066.

Davies, D.J., Ward, R.J., Heylings, J.R., 2004. Multi-species assessment of electrical resistance as a skin integrity marker for in vitro percutaneous absorption studies. *Toxicol In Vitro* 18 (3), 351–358.

EDETOX, 2000. Evaluations and Predictions of Dermal Absorption of Toxic Chemicals, EU Framework V: Quality of Life, Environment and Health Key Action Funding (Project Number: QLKA-2000–00196).

Fasano, W.J., Manning, L.A., Green, J.W., 2002. Rapid assessment of rat and human epidermal membranes for in vitro dermal regulatory testing: correlation of electrical resistance with tritiated water permeability. *Toxicol. In Vitro* 16, 731–740.

Flint, G.N., 1998. A metallurgical approach to metal contact dermatitis. *Contact Dermat.* 39, 213–221.

Franz, T.J., 1975. Percutaneous absorption on the relevance of in vitro data. *J. Invest Dermatol* 64, 190–195.

Fullerton, A., Hoelgaard, A., 1988. Binding of nickel to human epidermis in vitro. *Brit. J. Dermatol* 119, 675–682.

Hostynek, J.J., 2003. Factors determining percutaneous metal absorption. *Food Chem. Toxicol.* 41 (2003), 327–345.

Hostynek, J.J., Dreher, F., Pelosi, A., Anigbogu, A., Maibach, H.I., 2001. Human stratum corneum penetration by nickel: in vivo study of depth distribution after occlusive application of the metal as powder. *Acta Derm. Venereol. (Suppl.)* 212, 5–10.

Journey, W.S., Goldman, R.H., 2014. Occupational handling of nickel nanoparticles: a case report. *Am. J. Ind. Med.* 57 (9), 1073–1076.

Larese Filon, F., Boeninger, M., Maina, G., Adami, G., Spinelli, P., Damian, A., 2006. Skin absorption of inorganic lead and the effects of skin cleansers. *J. Occup. Environ. Med.* 48, 692–699.

Larese Filon, F., D'Agostin, F., Crosera, M., Adami, G., Bovenzi, M., Maina, G., 2009. In vitro absorption of metal powders through intact and damaged human skin. *Toxicol. In Vitro* 23, 574–579.

Larese Filon, F., Crosera, M., Adami, G., Bovenzi, M., Rossi, F., Maina, G., 2011. Human skin penetration of gold nanoparticles through intact and damaged skin. *Nanotoxicology* 5 (4), 493–501.

Larese Filon, F., Crosera, M., Timeus, E., Adami, G., Bovenzi, M., Ponti, J., Maina, G., 2013. Human skin penetration of cobalt nanoparticles through intact and damaged skin. *Toxicol In Vitro* 27 (1), 121–127.

Larese Filon, F., Mauro, M., Adami, G., Bovenzi, Crosera, M., 2015. Nanoparticles skin absorption: new aspects for a safety profile evaluation. *Regul. Toxicol. Pharmacol.* 72, 310–322.

Lidén, C., Carter, S., 2001. Nickel release from coins. *Contact Dermat.* 44, 160–165.

Lidén, C., Skare, L., Nise, G., Vahter, M., 2008. Deposition of nickel, chromium, and cobalt on the skin in some occupations – assessment by acid wipe sampling. *Contact Dermat.* 58, 347–354.

Magaye, R., Zhao, J., 2012. Recent progress in studies of metallic nickel and nickel-based nanoparticles' genotoxicity and carcinogenicity. *Environ. Toxicol. Pharmacol.* 34, 644–650.

Mauro, M., Crosera, M., Bianco, C., Adami, G., Montini, T., Fornasiero, P., Jaganjac, M., Bovenzi, M., Larese Filon, F., 2015. Permeation of platinum and rhodium nanoparticles through intact and damaged human skin. *J. Nanoparticle Res.* 17, 253.

Mazinanian, N., Hedberg, Y., Wallinde, I.O., 2013. Nickel release and surface characteristics of fine powders of nickel metal and nickel oxide in media of relevance for inhalation and dermal contact. *Regul. Toxicol. Pharmacol.* 65, 135–146.

Midander, K., Pan, J., Wallinder, I.O., Heim, K., Leygraf, C., 2007. Nickel release from nickel particles in artificial sweat. *Contact Dermat.* 56, 325–330.

Midander, K., Kettlerij, J., Julander, A., Lidén, C., 2014. Nickel release from white gold. *Contact Dermat.* 71, 108–128.

Patel, J.D., O'Carra, R., Jones, J., Woodward, J.G., Mumper, R.J., 2007. Preparation and characterization of nickel nanoparticles for binding to his-tag proteins and antigens. *Pharm. Res.* 24, 343–352.

Rui, F., Bovenzi, M., Prodi, A., Belloni Fortina, A., Romano, I., Corradin, M.T., Larese Filon, F., 2013. Nickel, chromium and cobalt sensitization in a patch test population in north-eastern Italy (1996–2010). *Contact Dermat.* 68, 23–31.

Sandt, J.J., Burgsteden, J.A., Cage, S., Carmichael, P.L., Dick, I., Kenyon, S., Korinth, G., Larese, F., Limasset, J.C., Maas, W.J., Montomoli, L., Nielsen, J.B., Payan, J.P., Robinson, E., Sartorelli, P., Schaller, K.H., Wilkinson, S.C., Williams, F.M., 2004. In vitro predictions of skin absorption of caffeine, testosterone, and benzoic acid: a multi-centre comparison study. *Regul. Toxicol. Pharmacol.* 39, 271–281.

Schmidt, M., Goebeler, M., 2011. Nickel allergies: paying the toll for innate immunity. *J. Mol. Med.* 89, 961–970.

Tanojo, H., Hostynek, J.J., Mountford, H., Maibach, H.I., 2001. In vitro permeation of nickel salts through human stratum corneum. *Acta Derm. Venereol. (Suppl.)* 212, 19–23.

Thyssen, J.P., Menné, T., 2010. Metal allergy – a review on exposure, penetration, genetics, prevalence, and clinical implications. *Chem. Res. Toxicol.* 23, 309–318.

Thyssen, J.P., Linneberg, A., Menné, T., Nielsen, N.H., Johansen, J.D., 2009. Contact allergy to allergens of the TRUE-test (panels 1 and 2) has decreased modestly in the general population. *Br. J. Dermatol.* 161, 1124–1129.

Thyssen, J.P., Gawkrödger, D.J., White, I.R., Julander, A., Menné, T., Lidén, C., 2012. Coin exposure may cause allergic nickel dermatitis: a review. *Contact Dermat.* 68, 3–14.

Wu, X., Xing, W., Zhang, L., Zhuo, S., Zhou, J., Wang, G., Qiao, S., 2012. Nickel nanoparticles prepared by hydrazine hydrate reduction and their application in supercapacitor. *Powder Technol.* 224, 162–167.